



BASELINE STUDY OF THE RANGITATA RIVER MOUTH ENVIRONMENT

Caitlin Frazer, Livvy Harris, Sophie Newsham, Jordan Ballisat,
Dennis Fogarty

Contents

1. Executive Summary.....	2
2. Introduction	3
3. Literature Review	4
3.1 Introduction to hāpua and controlling processes	4
3.2 Management of Coastal Environments	6
3.3 Common Methodological Processes.....	6
4. Methodology.....	7
4.1 Aerial and Satellite Imagery	7
4.2 Beach Profiles	7
4.3 Wave Data.....	8
4.4 River flow and rainfall	8
5. Results	9
5.1 Long-term Trends	9
5.1.1 Images	9
5.1.2 Beach Profiles	12
5.2 Short-term Trends	16
5.2.1 Imagery	16
5.3 Analysed Controlling Factors	20
6. Discussion	20
6.1 Hāpua morphology.....	20
6.2 Variability of the middle beach profiles	22
6.3 Accretion.....	23
6.4 Erosion	24
6.4.1 Cut back into bank	24
6.4.2 Erosion south of the river mouth	25
6.5 River Flow Influence	25
6.5.1 Flood Events	25
6.5.2 Low flow events.....	26
6.7 Outlet migration.....	27
7. Limitations	27
8. Conclusion	27
9. Further research	28
10. Acknowledgements.....	28
11. Appendices.....	29

1. Executive Summary

Context

- The Rangitata River mouth environment is located along the Canterbury Bight, on the South Island of New Zealand. It is characterised by a mixed sand and gravel coastline, and a hāpua. Environment Canterbury (ECan) has requested a baseline of the geomorphic variability to be established. This report will be used by ECan to compare geomorphological changes as part of adaptive management approaches, to prepare for the impacts of climate change and increased water abstraction.

Research Question

- What is the geomorphic variability of the Rangitata River mouth environment for future comparisons?

Methods

- The methods for this report were based on secondary data analysis. These focused on:
 - Satellite & aerial imagery (1937- 2020)
 - Wave buoy data (1999 - 2019)
 - River flow data (1979 - 2020)
 - Beach profiles (1986 - 2019)

Key Findings

- River outlet is dynamic but tends to be located northeast.
- Southerly waves potentially cause northern migration of the outlet channel.
- Easterly waves tend to cause short, dramatic changes to the shoreline.
- High flow events cause significant change to the river outlet position and bar shape.
- During low flows, it is more common to see the hāpua separated from the main river flow.
- Beach profiles are highly dynamic with periods of erosion and accretion, as well as formation of a secondary channel.

Limitations

- The key limitations were time constraints, irregularity, and gaps in the data, poor image resolution, human error, and difficulties corresponding data. Other limitations included the position of the wave buoy and river gauge and the unknown effect of the abstraction rate on the environment.

Further Research Suggestions

- A deeper analysis into longshore drift, wind, tides, tectonic uplift, erosion rates, and sediment type and volume.
- Installation of a webcam to get high quality daily data for a more consistent record.
- Identify the potential impacts of climate change induced sea level rise, river flow, and wave effects on the environment.

2. Introduction

Globally, river mouths are important for their economic, cultural, ecological, and recreational values (Kirk, 1991). The river mouth environment at the Rangitata River is complex with the dominant feature being a hāpua (Figure 1). Hāpua are common throughout the east coast of the South Island, New Zealand (NZ), although the Rangitata Hāpua is understudied (Hart, 2009). Understanding the dynamics of this environment is important due to potential hazards from floods and sea level rise (Hart, 2009; Kirk & Lauder, 2000). Significant amounts of water are abstracted from the Rangitata River and increases have been proposed. This means it is important to understand dynamics of the river mouth environment if the increase in water abstraction causes changes (Hart & Bryan, 2008).

This baseline study, proposed by Environment Canterbury (ECan), aims to build a historic picture of the variability in the geomorphology at the Rangitata River mouth environment (RRME). The research question is what is the geomorphic variability of the RRME for future comparisons? This report will commence with a brief review of the key literature, then describe the methods used, followed by results and discussion.

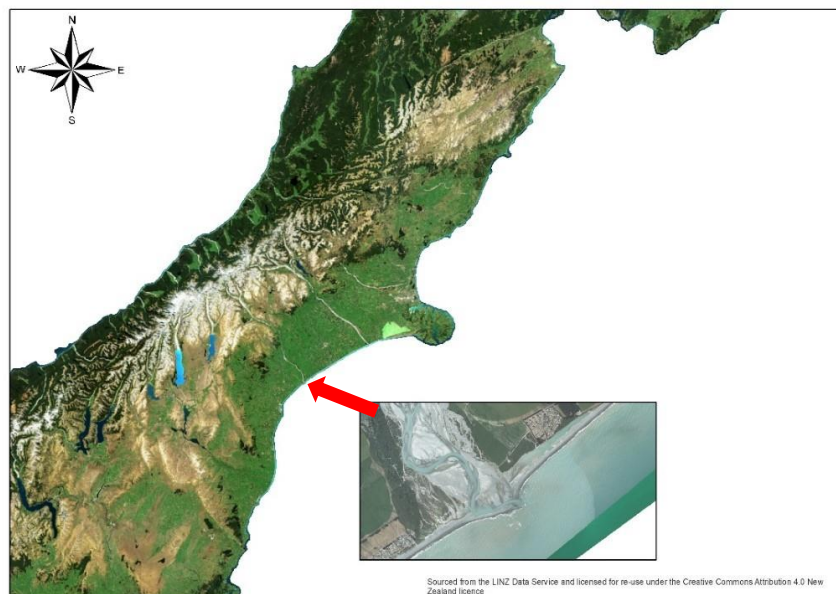


Figure 1. Map indicating location of study. Images sourced from LINZ Data Service and Canterbury Maps.

3. Literature Review

3.1 Introduction to hāpua and controlling processes

Braided rivers that terminate at a wave-dominated mixed-sand and gravel coastline (Appendix (Apx.) A), form a specialised setting, which in NZ are referred to as hāpua. These are elongated lagoon environments and consist of non-estuarine bodies of water that are semi-enclosed by a barrier bar (Kirk, 1991; Kirk & Lauder, 2000; Paterson et al., 2001). Freshwater from the river enters the ocean via an outlet channel and seepage through the permeable bar (Hart, 2009).

Globally hāpua are understudied, although there are detailed and broad studies on hāpua in Canterbury. Specific studies on the Rakaia (McHaffie, 2010), Ashburton (Paterson et al., 2001), and Hurunui Hāpua (Measures et al., 2020) have been completed. While the only study on the Rangitata Hāpua was completed 22-years ago (Todd, 1998). Therefore, further research of the RRME is required.

Sediment transport and hydrological effects, driven by fluvial and marine physical processes, control the geomorphology of river mouths (Kirk, 1991; Hart, 2009). Variations in river flow change the sediment transport and erosional rate while sea storm events, swash, and cross-shore sediment exchange are the major marine processes that drive changes within hāpua (Hart, 2009; Kirk 1991). The combination of these processes causes the most significant changes at the mouth (Figure 2).

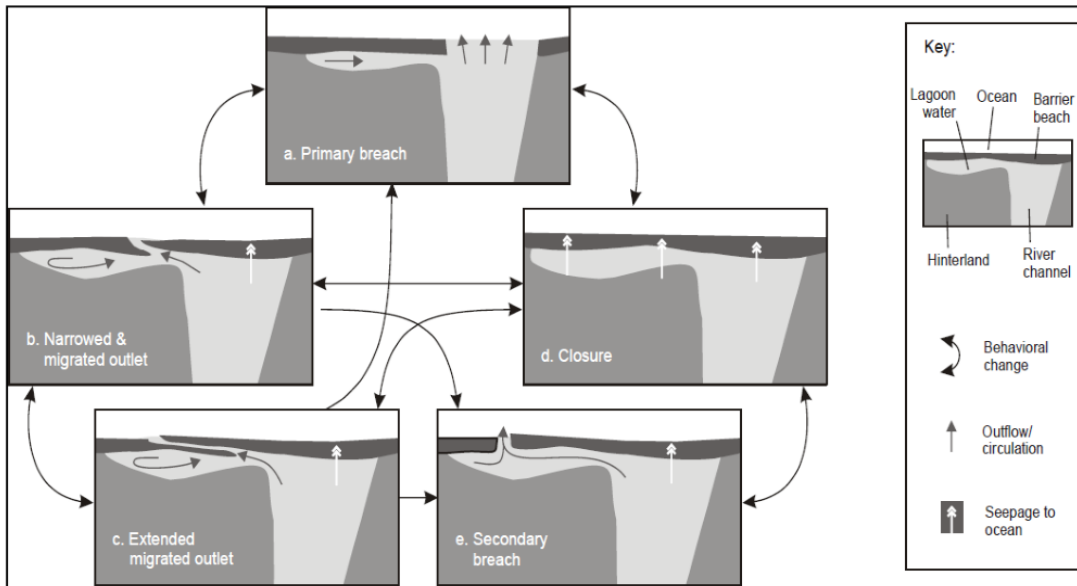


Figure 2. A flow diagram composed by Hart, 2009 of the common morphological stages observed in Canterbury rivers mouths such as the Opihi, Ashburton, Hurunui, Rangitata, Rakaia and Waitaki. A Primary breach (a) is mostly associated with high flow events and can sometimes occur due to high waves. Whereas a secondary breach (e) can occur during moderate floods as the migrated and elongated outlet is truncated. The combination of the outlet migration (b) and channel elongation (c) is attributed to low to moderate flow events and the longshore transport direction. Lagoon closure (d) would result from low river levels combined with low-high energy waves on the

Fluvial processes are dominant influencers of geomorphology of large river mouths (Kirk, 1991). Understanding the influence these processes have is important due to management implications (Kirk, 1991). At least 7 m³/s of water has been diverted from the Rangitata River since 1945, which may affect the RRME through reduced flow (Hart & Bryan, 2008). Changes in river flow affect sediment supply and remobilisation (Masselink et al., 2014). Flooding events have the greatest impact on river mouth morphology (Kirk, 1991; Masselink et al., 2014). Rivers with higher base flows frequently breach the barrier bar due to flooding (Hart & Bryan, 2008). This breaching often changes outlet location and causes a sediment injection into the marine environment (Hart & Bryan, 2008). While low flow events have less significant impacts on morphology, they can cause bar and hāpua closures (Kirk, 1991).

The dominant marine processes controlling river mouth morphology are waves and longshore currents (Hart & Bryan, 2008; Kirk, 1991). Waves remobilise and transport sediments on the shoreface (Hart, 2007; Todd, 1998). Wave approach can influence outlet channel location and angle, while wave height can influence channel width (Hart & Bryan, 2008; Kirk & Lauder, 2000; Measures, 2020). Common wave direction in the Canterbury Bight is south to north

(Pickrill & Mitchell, 1979). This generates a northern longshore current which has created the barrier bar at the RRME (Hart, 2009).

Research suggests that hāpua in Canterbury are experiencing “long-term net erosional retreat” (Kirk & Lauder, 2000, pg. 14). Estimated erosion rates range from 0.3 to 1.5 meters per year (Eikaas & Hemmingsen, 2006; Gabites, 2005; Single, 2011). However, Hart (2009) believes that landward shores of hāpua may not be keeping pace with barrier erosion; therefore, hāpua surface areas are decreasing.

3.2 Management of Coastal Environments

Appropriate management of hāpua is important due to hazards, ecological, and cultural values (Hart, 2007). The settlement adjacent to the RRME known as the Rangitata Huts could experience loss of land due to coastal erosion. Mana whenua have cultural values regarding the natural character of water bodies to supply food and recreational activities (Williams, 2006). Developing understandings of river systems allow Māori to employ specific management strategies (Ulluwishewa et al., 2008).

Coastal management in NZ means coastal features are managed separately from upstream environments that influence them (Hart, 2009). This means that the Rangitata River is being managed without consideration of the effect on the RRME. This indicates the importance of this study, as increased water abstraction upstream is being proposed without an understanding of the current geomorphic variability of the RRME.

3.3 Common Methodological Processes

The rare nature of hāpua cause difficulties in determining the best approach for analysis due to limited research. Methods of historical data analysis are commonly based on sand beaches, or other water bodies such as lagoons. Therefore, the following methods should be used cautiously within this study.

Studies commonly use satellite imagery, to analyse short-term geomorphological changes. Whereas longer-term temporal analysis of variation in a shoreline incorporates numerous sources of data such as aerial and topographic maps and beach profiles (Ayadi et al. 2016; Do

et al. 2019; Marfai et al. 2008; Ozturk & Sesli, 2015). This is beneficial as they have a wide range of data and may have better results.

4. Methodology

4.1 Aerial and Satellite Imagery

ArcMap was used to analyse and digitise the imagery. This allowed layers of images and feature classes to be compiled. Digitisation methods include creating line and polygon features. Polygons were used when analysing flood events, while lines were used in determining long-term trends. Furthermore, measuring tools in ArcMap and Google Earth Pro was used to establish measurements of features.

The satellite imagery used was sourced from Planet Labs, which provided images from 2016. The basemap used for georeferencing was a high-resolution Canterbury Maps image taken in February 2019. Historical aerial images were used to display long-term trends. These were sourced from Retrolens, which provided one image roughly every 10-years. Google Earth Pro images were also studied and had irregular images from 2006. These were higher quality than Planet Labs but often the dates did not correspond with notable events from river flow or wave data.

4.2 Beach Profiles

Beach profile surveys have been completed by ECan across five sites in the RRME (Figure 3). Matlab was used to create beach envelopes, and subplots for the four northern profiles, which were used to identify trends in geomorphic variability. Matlab was also used to calculate sediment volumes at each site. Time series graphs created in Microsoft Excel (ME) showed changes in sediment volume. ME was used to create excursion plots for the profile sites.

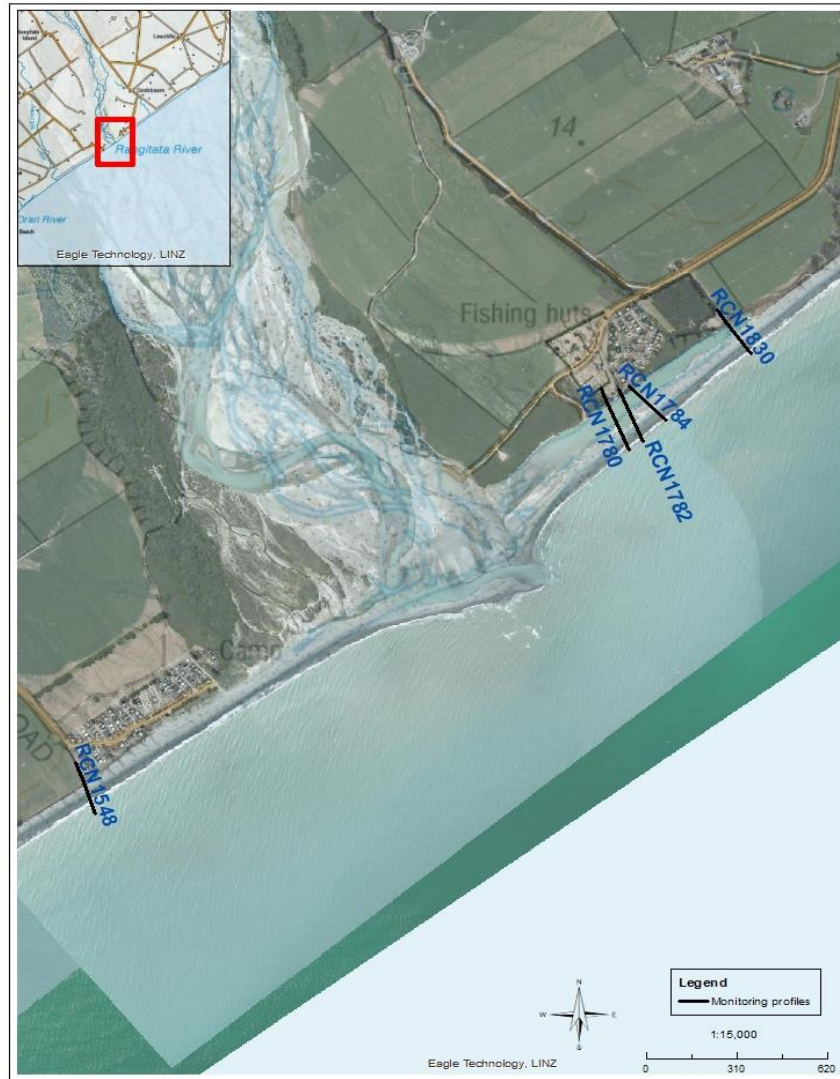


Figure 3. Map showing the location of the five beach profile sites. There is one south of the river mouth and four to the north. The four northern ones run through the hāpua.

Image sourced from ECan.

4.3 Wave Data

Wave data was collected by ECan from a buoy 17 kilometers east of Banks Peninsula. The wave data record was from 1999 to 2019. ME was used to create tables, histograms, scatter plots, and bar charts to identify significant wave height and wave direction. Once geomorphic changes were identified through imagery, wave data for similar time periods was analysed.

4.4 River flow and rainfall

The river flow and rainfall data were supplied by ECan. The rainfall gauge records daily precipitation 120km upstream of the RRME. Data was recorded since 2010. River flow data

was recorded 60km upstream of the RRME over 41-years. Both data sets were analysed using ME to create summary tables, bar charts, and scatter plots for trend identification. This data was used alongside imagery analysis to investigate high flow and low flow events.

5. Results

5.1 Long-term Trends

5.1.1 Images

Analysis of the last 80-years of imagery, shows variation in river outlet position, width, and angle to the coast (Figure 4). The outlet is predominantly northeast of the river channel, except during 1967, 1987, and 1998 when it is southeast of the river channel. Moreover, the position of the hāpua varies from south and north of the river mouth.

There were differences in trends over the last 10-years of imagery compared to the last 80-years (Figure 5). The outlets tend to be in the northeast portion of the RRME, while the hāpua is not observed south of the river mouth since 1976.

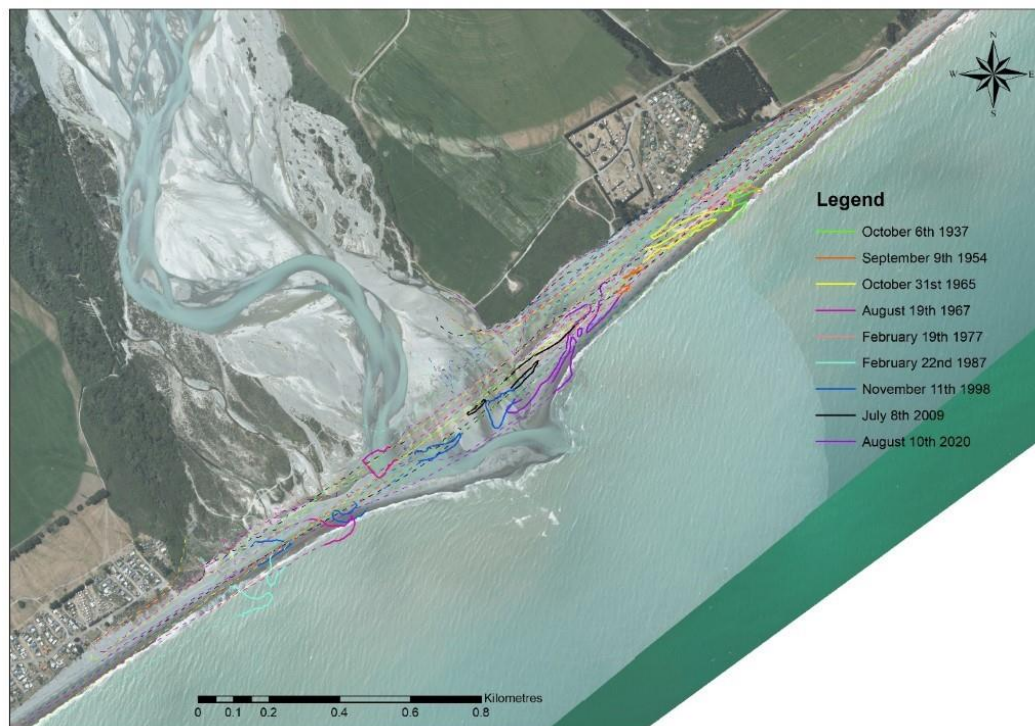


Figure 4. Map of the long-term trends (1937-2019), with around 10-year intervals between years. The rare years when there was also a hāpua in the south-east were 1954, 1965, and 1976. This was created in ArcMap, incorporating Retrolens, Google Earth, and Planet Labs imagery. Bold lines represent the river outlet, while the dashed lines outline the shorelines. Basemap is February 2019 Latest Aerial Imagery from Canterbury Maps.

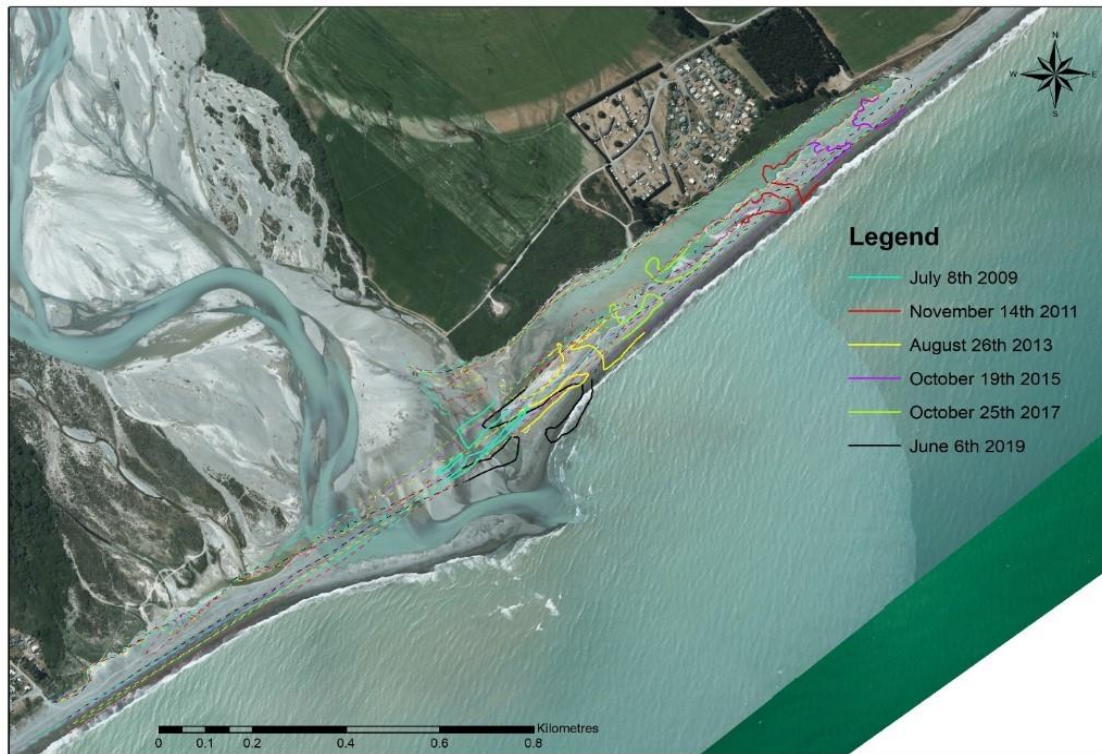


Figure 5. Map of the latest trends (2009-2019), with 2-year intervals between years. This was created in ArcMap, incorporating Google Earth and Planet Labs imagery. Bold lines represent the river outlet, while the dashed lines outline the shorelines. Basemap is February 2019 Latest Aerial Imagery from Canterbury Maps.

Quantifying the morphological changes of the hāpua (Table 1 and 2) showed that the hāpua is decreasing in length but increasing in area over the last 80 years. During the last 10-years the hāpua has remained relatively stable, although the amount it extends past the northern huts forest line has receded by ~130m.

Table 1. Table of the long-term measurements taken from the RRME long term imagery. Note: Values are rounded to the nearest 10m to account for error.

Year	Hāpua Length	Hāpua Area	Extending past the forest line at the northern end of huts	Other observations
1937	1415m	81,330m ²	390m	
1954	1280m	67,075m ²	530m	Southern hāpua
1965	1670m	61,800m ²	190m	Southern hāpua
1977	1230m	80,070m ²	85m	
1987	805m	30,960m ²	45m	Northern hāpua cut off from the river channel. Southern outlet.
1998	940m	38,080m ²	30m	Two outlets, one southern & one central.
2009	1185m	72,740m ²	60m	
2020	1060m	61,070m ²	50m	
Average	1200m	61,640m²	175m	

Table 2. Table of the latest trend measurements taken from the RRME over the past 10 years. Note: Values are rounded to the nearest 10m to account for error.

Year	Hāpua Length	Hāpua Area	Extending past the forest line at the northern end of huts
2009	1180m	74,700m ²	52m
2011	1140m	62,100m ²	35m
2013	1035m	70,620m ²	30m
2015	1095m	91,770m ²	32m
2017	1125m	75,350m ²	34m
2019	1170m	81,070m ²	91m
Average	1125m	75,935m²	45m

5.1.2 Beach Profiles

The southern beach profile envelope (RCN1548) (Apx. B1) shows that the site has been extremely dynamic from 1981 to 2019. However, from 1989 the site has been in an erosional state (Figure 6), which has also resulted in decreasing sediments volumes (Figure 7).

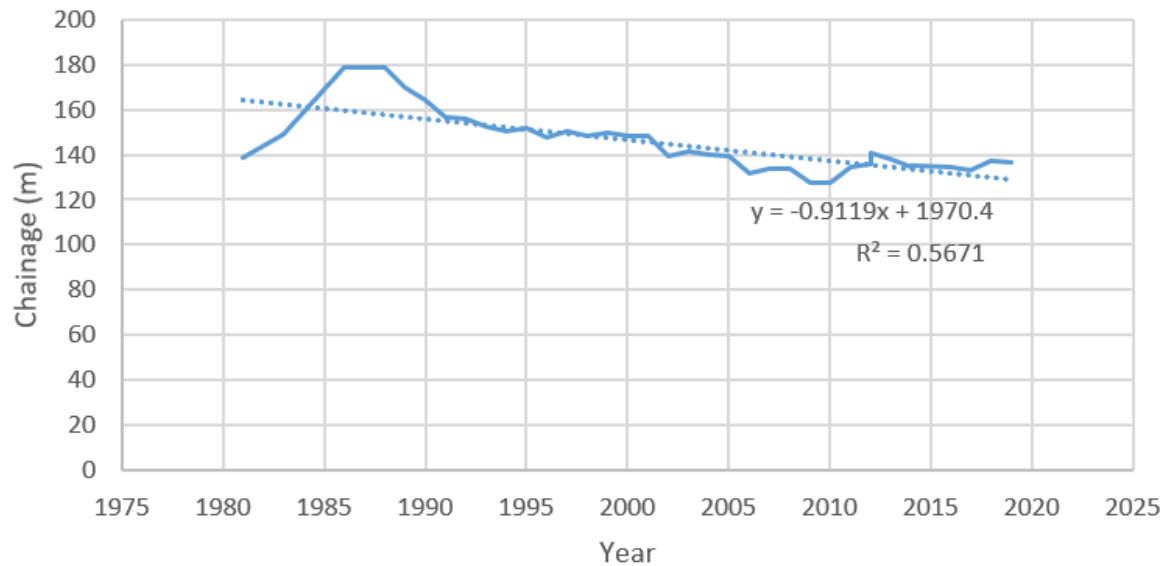


Figure 6. This excursion plot shows a short accretionary period from 1981 to 1988. Then the beach has been in an erosional state from 1989 to 2019. This erosional trend is also shown by the negative trendline and the R-squared value of 0.57 which shows a reasonable strong relationship. Data sourced from ECan.

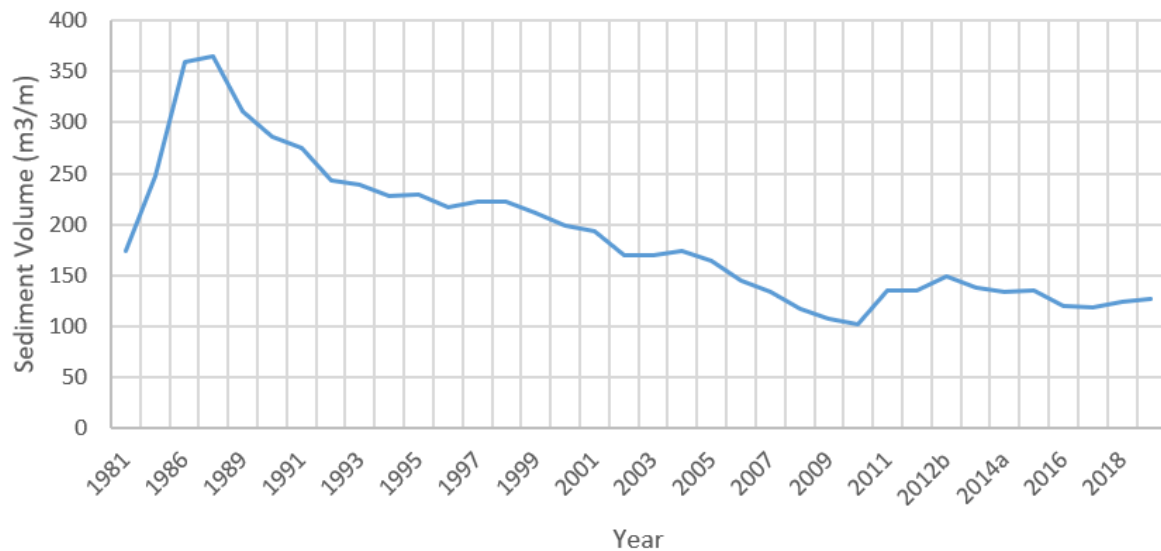


Figure 7. Changes in sediment volume at RCN1548. The peak sediment volume at the end of the short accretionary period was 365.4 m³/m. This had decreased to 126.89m³/m in 2019. Data sourced from ECan.

The middle three profile sites (RCN1782, RCN1780 and RCN1782) showed the same trends so only one (RCN1782) will be referred to here. The beach envelope for 1993 to 2019 (Figure B2) shows that RCN1782 is a dynamic site which has experienced changes in the shape of the profile. The formation of a secondary bar at this site occurred in 1998 and persisted until 2005 (Figure 8). This site has had distinct periods of erosion and accretion (Figure 9), which is also shown by changes in sediment volume (Figure 10).

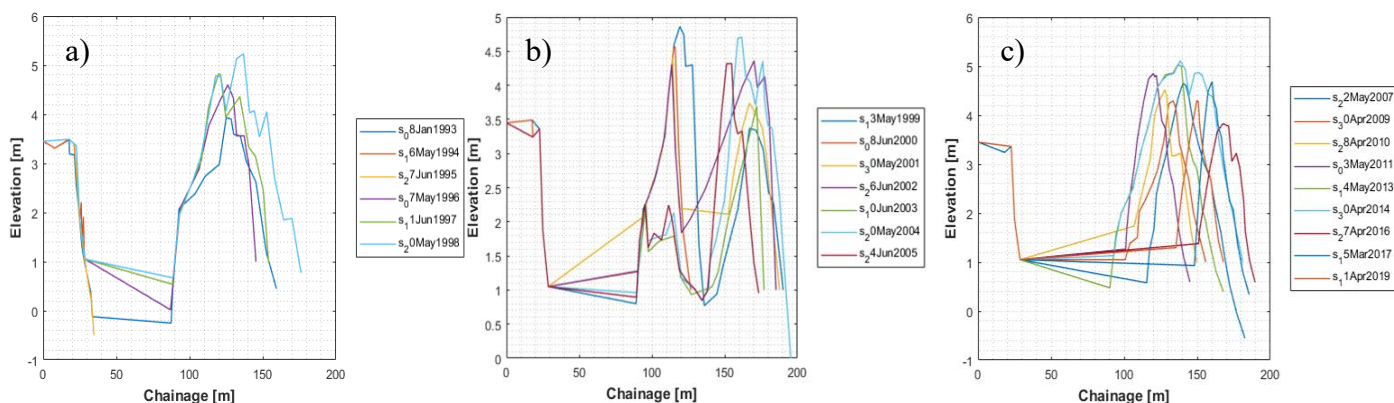


Figure 8. Profiles for site RCN1782 showing changes in shape. a) illustrates one main channel, which is the hāpua, and one bar feature. b) shows the formation of a secondary bar between approximately 150m to 200m. c) shows the change back to the only one bar. Data sourced from ECan.

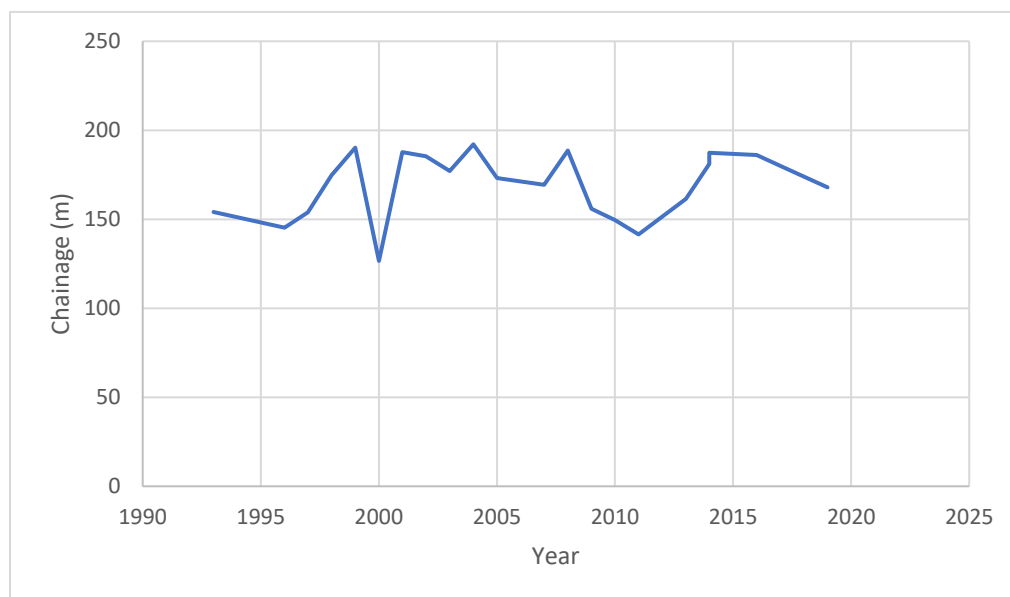


Figure 9. Excursion plot for RCN1782. There are clear periods of erosion and accretion, however, no long-term trend is visible. Data sourced from ECan.

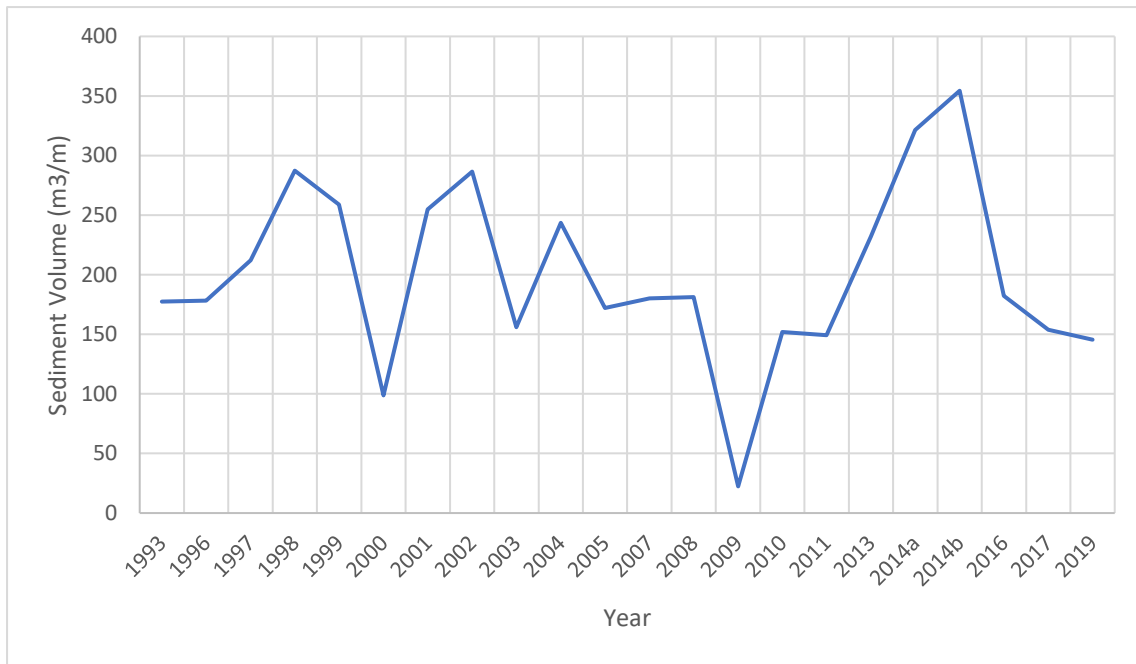


Figure 10. Time series showing changes in sediment volume for RCN1782. There are clear periods of erosion and accretion, however, no long-term trend is visible. Data sourced from ECan.

The northern profile site (RCN1830) has been a highly dynamic location from 1986 to 2018 (Figure B3). The formation of a secondary bar feature is also a common occurrence at this site (Figure 11). There have been periods of erosion and accretion however, a long-term trend of accretion can be identified (Figure 12). This same pattern is shown by changing sediment volumes from 1986 (Figure 13). There has also been a widening of the main barrier bar feature (Figure 14).

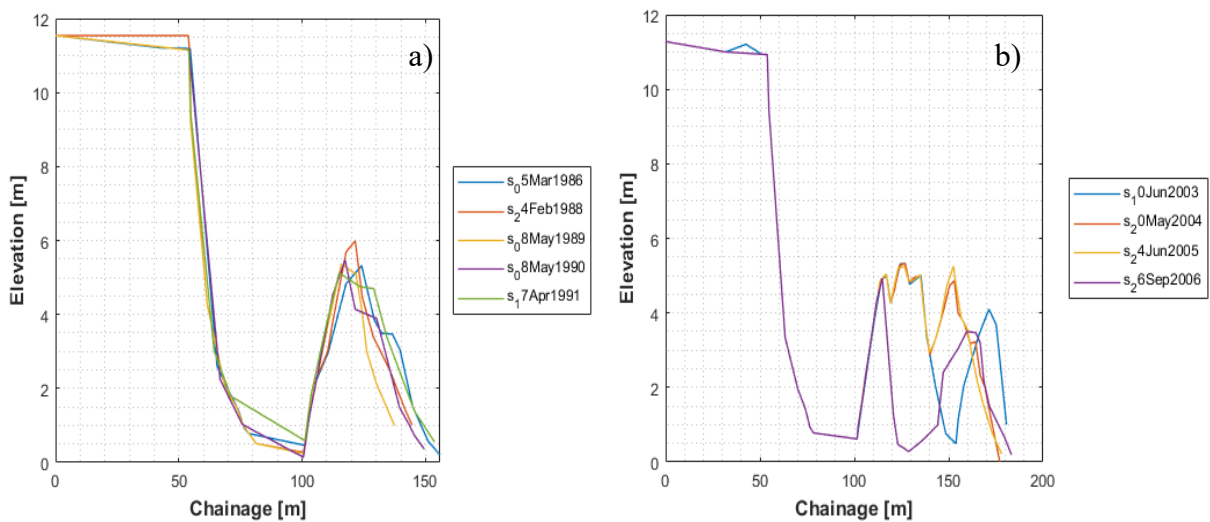


Figure 11. Profiles showing examples of different shapes identified at RCN1830. a) shows one main channel, which is the hāpua between 1986 and 1991, and one bar feature. b) shows the formation of a secondary bar between approximately 150m and 200m. Data sourced from ECan.

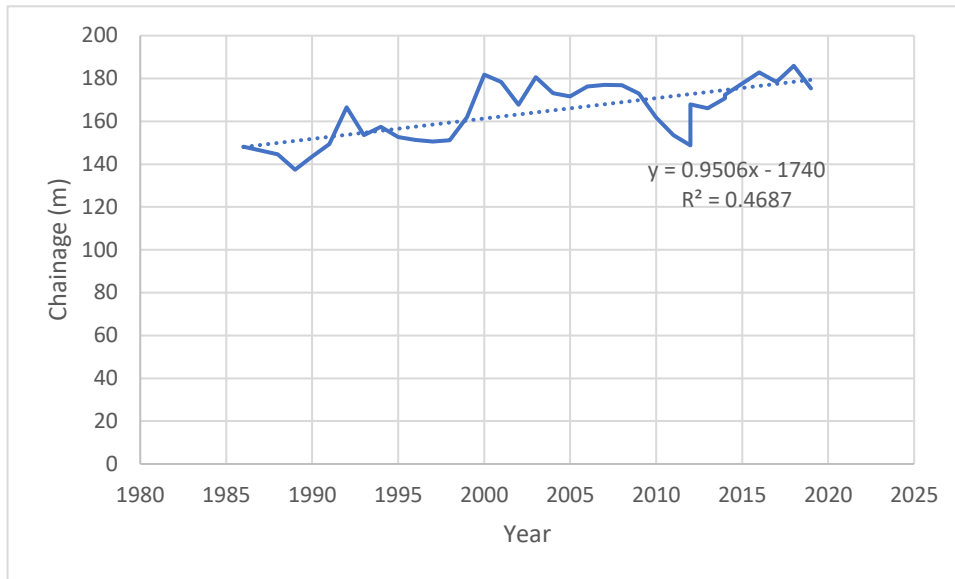


Figure 12. Excursion plot for RCN1830. There have been periods of erosion and accretion, but there has been a long-term trend of accretion. This is demonstrated by the positive trendline and R-squared value of 0.47. Data sourced from ECan.

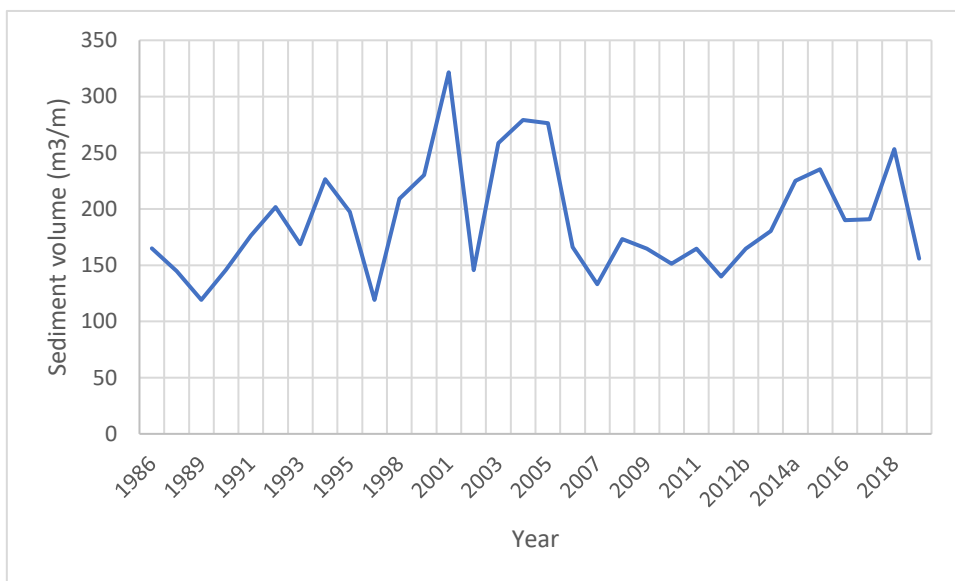


Figure 13. Changes in sediment volume for RCN1830. There have been distinct periods of erosion and accretion, but no long-term trend visible. Data sourced from ECan.

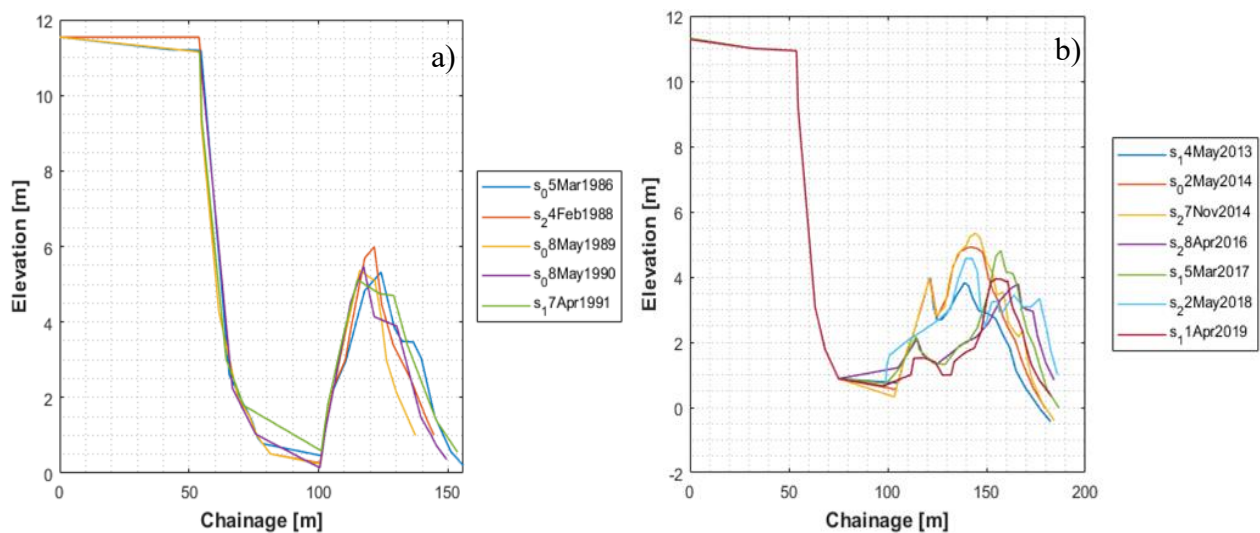


Figure 14. Profiles for RCN1830 showing widening of the barrier bar. The width was approximately 50m from 1986 to 1991 (a), and between 2013 and 2019 it was approximately 80m (b). Data sourced from ECan.

5.2 Short-term Trends

5.2.1 Imagery

Analysis of the five largest flood events from 2016-2020 showed similar trends. This time period was chosen because there was access to near-to daily imagery. The dominant morphological patterns were widening of the outlet channel, seaward movement of the bars near the outlet (Figure 15) and breaching of the barrier bar directly downstream of the main river flow (Figure 16) (see Apx. C for further detail).

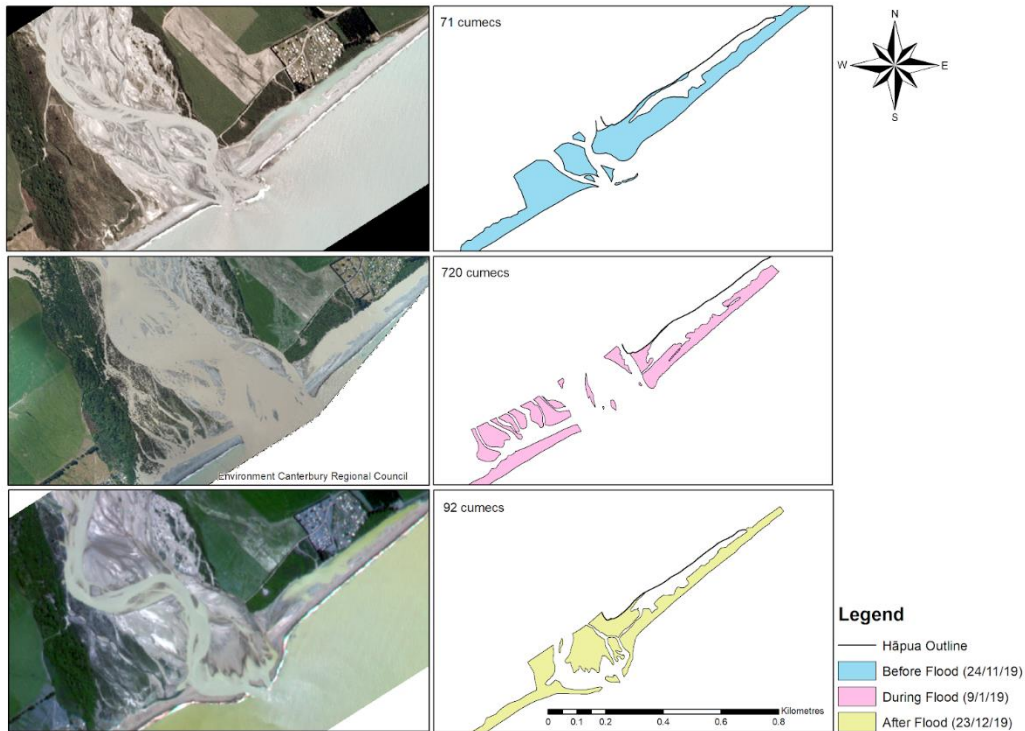


Figure 15. This sequence of images and polygons represents a flood event in November 2018 of 1847m³/s. The blue polygon represents where the bars were prior to the flood while the pink represents the bars during the flood. It is illustrated in the yellow polygon that after the flood the bars either side of the outlet moved seaward in a convex shape.

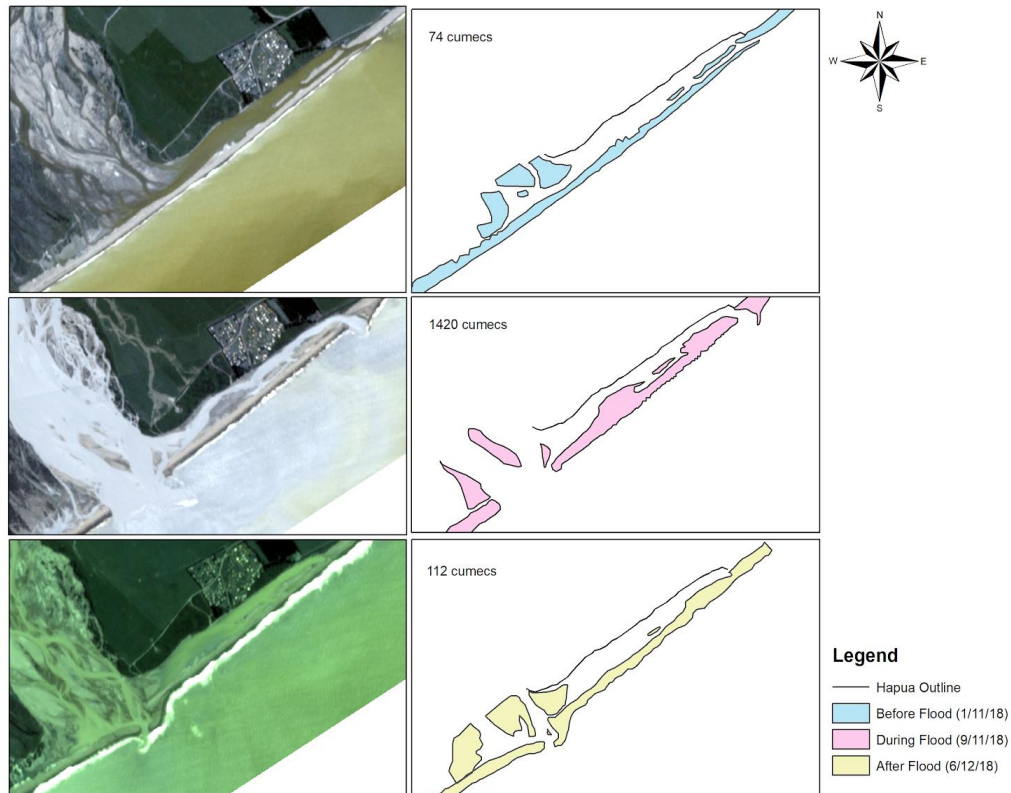


Figure 16. A sequence of prior, during and after a flood event in November 2018 of maximum 1847m³/s. The coloured polygons represent the bar features. Images sourced from Planet Labs.

Images since 2016 with corresponding river flows of less than 70m³/s indicates that the hāpua can separate from the main river flow for up to days at a time (Figure 17). There was no clear evidence to show full barrier bar closure.

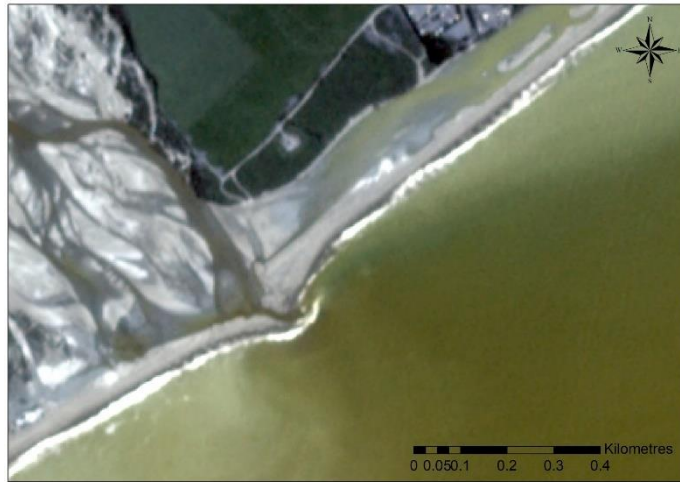


Figure 17. A false-colour image indicating a time period when the hapua is separated from the main river flow. The river flow was ~65m³/s on average for the date of 19th of February 2019. Image sourced from Planet Labs.

Episodes of northern outlet migration were observed and commonly followed a flood event (Figure 18). Faster migration occurred initially after a flood as opposed to when the outlet was adjacent to the middle of the hāpua.



Figure 18. This series of false colour maps shows northern outlet migration. The measured distance between image 1 and 2 is $170\text{m} \pm 10\text{m}$ which represents on average 14m per day over this time period. The distance measured between image 2 and 3 is $60\text{m} \pm 10\text{m}$ which represents on average less than 3m of migration per day. The distance measured between image 3 and 4 was $520\text{m} \pm 20\text{m}$ which represents on average 8m per day. Overall, the outlet moved north-east $\sim 800\text{m}$ over the four-month period. Images sourced from Planet Labs.

Over the past 11-years significant erosion has occurred southeast of the Rangitata Huts (Figure 19). The yellow line represents the shoreline of the hāpua in 2009, while the red is 2019. This erosion was estimated to be $\sim 35\text{m} \pm 10\text{m}$ using measurement tools in ArcMap.



Figure 19. Map of the erosion into the bank SE of the Rangitata

5.3 Analysed Controlling Factors

The dominant processes influencing RRME geomorphology are river flow and wave approach. Analysis of wave and river flow data showed that there were a range of long-term and short-term trends.

Wave analysis showed dominant wave direction is from the south (Apx. D). There was variation in wave heights with an average significant wave height of 1.5m (Apx. D). There were also occasions of high easterly waves, which may also control geomorphology at the RRME.

The river flow data shows no long-term trends for average high flows or average low flows, although a negative trend is illustrated in the annual average flow. The average monthly flow shows a seasonal trend with increased flow in the summer months, due to glacial melt and tropical cyclones (see Apx. E for further information). Flood events can reach as high as 2800cm³/s and can be associated with high rainfall (Apx. F shows associated graphs).

6. Discussion

6.1 Hāpua morphology

Models composed by Todd (1998) and Hart (2009) (Figure 2) are comparable to what was observed at the RRME (Figure 20). Links can be made with these morphological stages to both river flow and wave conditions. An increase in river flow can cause primary and secondary breaching of the barrier bar as the flow overtops the bars (Figures 18 & 19)(Apx. F). While the northern longshore current is the probable driver for the northern outlet migration and elongation (Figure 21)(Apx. D3) (Hart, 2009; Kirk 1991; Todd 1998). Generally, the outlet is wider when it is in a southern or central position (Apx. G). This was associated with high flow events and recent breaches, while outlet narrowing and elongation with near-parallel alignment to the coastline was associated with low flows. This corresponds with prior research (Hart, 2009; Todd, 1998). Low flow events can also cause hāpua and bar closures (Figure 17) (Todd 1998). Although no bar closures were observed in this research, it is still a possibility.

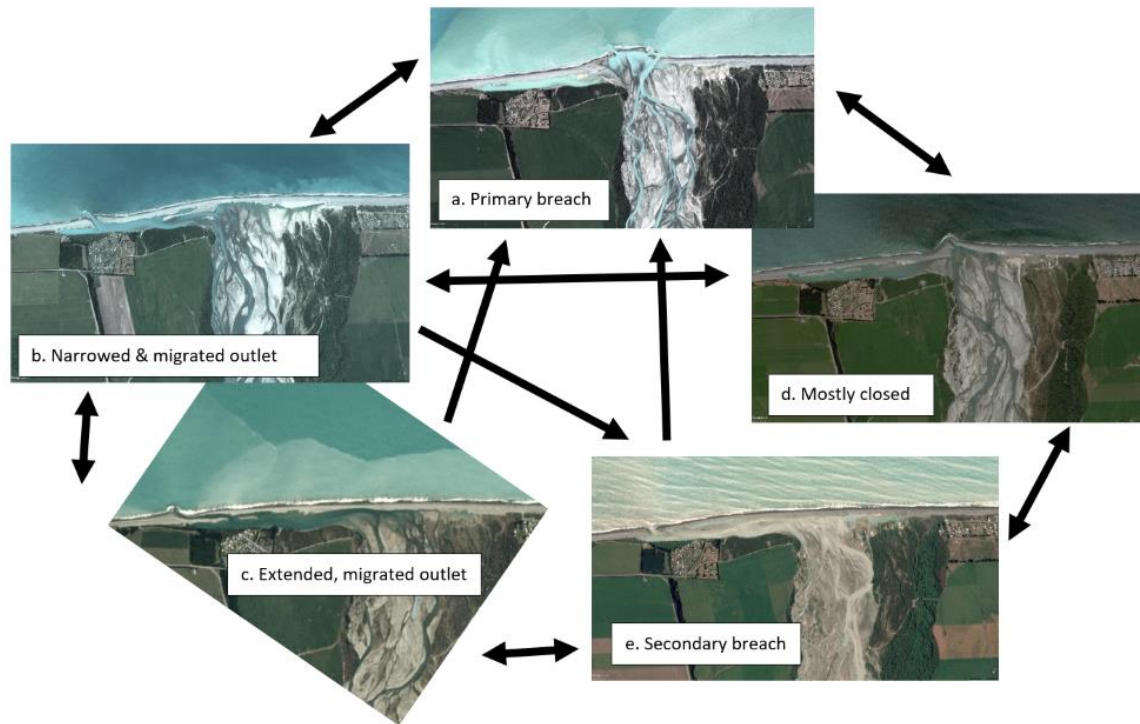


Figure 20. A flow diagram illustrating the stages of commonly observed morphology of the RRME. Adapted from Hart, 2009 pg. 1357.

The long-term imagery analysis found that the hāpua is more commonly located northeast of the river (Figures 4 and 5) which was also noted by Kirk (1991) and Todd (1998). However, there were instances of a second hāpua in the south before 1976. No links with river flow or wave data were obtained but a possible reason for this is the location of the main river flow further south than it is today (Figure 21).



Figure 21. Image of the RRME showing extinct river channels further south of the main flow than in more recent years which could explain the hāpua position south of the river mouth in previous years such as 1954, 1965, and 1976. Images sourced from Google Earth Pro and was taken on the 8th of July 2009.

The Rangitata Hāpua has been decreasing in water surface area and length over the examined images (Table 1). It was observed that the length of the hāpua was at its longest in 1937. This was prior to water abstraction. The water abstraction has likely had an impact on the morphology of the RRME (Hart & Bryan, 2008), but there is insufficient data before 1945 to make a clear connection.

The decrease in the size of the hāpua could align with Hart's, (2009) interpretation that the landward shores of hāpua are not eroding as quickly as the associated barrier bars. Erosion may cause the bars to shift landward at a greater rate than the bank is eroding. Moreover, Measures et al. (2020) states that the current models for similar river mouth environments do not account for the long-term erosion seen at retreating coastlines. The current baseline for the RRME is that the hāpua size is in decline but further research is needed for rationalization.

6.2 Variability of the middle beach profiles

RCN1782 has experienced erosional and accretionary periods, but no long-term trend (Figures 9 and 10). A possible reason for these dynamics is El Niño Southern Oscillation (ENSO). ENSO is a multiyear oscillation, consisting of two phases, which effects climatic processes on a global scale (Christopherson & Birke, 2015). During phases of El Niño high-pressures persist in the Western Pacific causing increased rainfall over the West Coast of NZ (NIWA, n.d.). However, when comparing erosional periods for RCN1782 to the Southern Oscillation Index (SOI) no obvious links between phases can be identified (Australian Government Bureau of Meteorology, 2020). Figure 22 shows the monthly SOI from 1996 to 1998, during this time there were two La Niña occurrences and one El Niño. However, from 1996 to 1998 RCN1782 was accreting and the sediment volume increased by 108.86m³/m. This indicates that moving between El Niño and La Niña had no impact on moving between erosional and accretional periods at RCN1782. However, the profiles were only taken annually, so if more regular data had been collected then the effects of ENSO may have been identified.

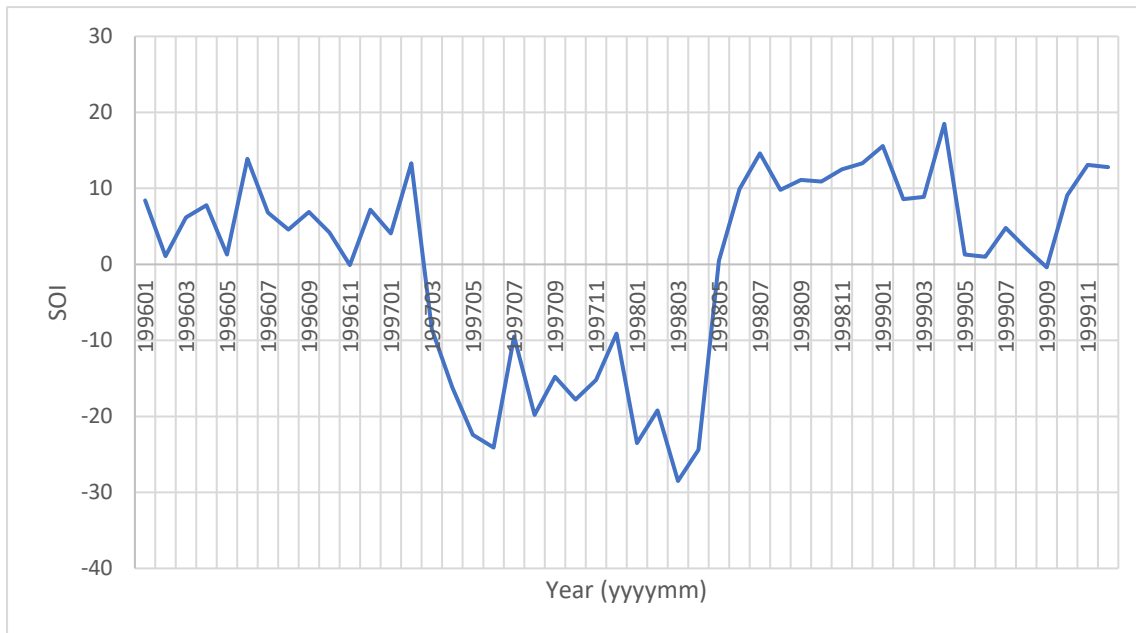


Figure 22. SOI from 1996 to 1999. When there are sustained periods of +7 or above this indicates La Niña. Whereas sustained periods of -7 indicate El Niño. Data sourced from Australian Government Bureau of Meteorology.

Another key trend identified for RCN1782, is the formation of a secondary bar between 1999 and 2005 (Figure 8). However, due to no imagery for this time period and annual collection of profile data the causes of this feature have not been investigated. Furthermore, the formation of the secondary bar doesn't coincide with any significant increases or decreases in sediment volume. The mean sediment volume between 1993 and 1998, when there was only one bar, was 213.8m³/m. Whereas between 1999 and 2005 the mean sediment volume was 210.08m³/m. Although this research was unable to identify any causes for the dynamics at RCN1782, they still need to be incorporated into a baseline and can be an area for further research.

6.3 Accretion

The coastline north of the RRME (RCN1830) has experienced an overall trend of accretion since 1986 (Figure 12). The trend of net accretion is contrary to what is expected according to the Department of Conservation (2000) who suggests that hāpua will roll back. This means that a hāpua would maintain its morphology but would move in a landward direction in response to rising sea levels. However, the results from this study found that RCN1830 is

accreting. This is similar to results found by McHaffie (2010), in her study of the Rakaia Hāpua, as the barrier bar moved seaward from 1952 to 2004.

RCN1830 has also displayed a widening of the barrier bar (Figure 14). This is supported by long-term accretion and increases in sediment volumes. The mean sediment volume between 1986 and 1991 was 150.23m³/m, which increased to 203.34m³/m between 2013 and 2019. This is most likely due to the influence of the northern longshore current in this region (Figure 23). The accretionary trend and widening of the barrier bar occurring at RCN1830 are important elements to incorporate in a baseline of the RRME.



Figure 23. Aerial image showing long-shore transport of sediment in a south to north direction, indicated by red arrow. This is moving sediment away from the southern end of the RRME and towards the northern end, which could be contributing to erosion in the south and accretion in the north. Image sourced from *Planet Labs*.

6.4 Erosion

6.4.1 Cut back into bank

There was an estimated ~35m of erosion into the bank southeast of the Rangitata Huts (Apx. H). This occurred over a period of 10-years and is likely due to the hāpua as well as the river channel interacting with the bank (Todd 1992; Measures et al. 2020) (Figure 24). Hāpua often erode into this landward shoreline, which is classified as lagoon retreat (Kirk & Lauder as cited in Hart, 2009). Over the last century, the hāpua hardly eroded the landward shore (Hart, 1999; Todd, 1998), which means that the erosion rate has accelerated in the past 10-years. In terms of long-term trends, as the hāpua backshore continues to erode, it should experience the same rate of erosion as the adjacent shoreline on the coast (Todd, 1992; Measures et al.

2020). The erosional distance between the 2-yearly images tends to be around 10m at its greatest point (Apx. H)

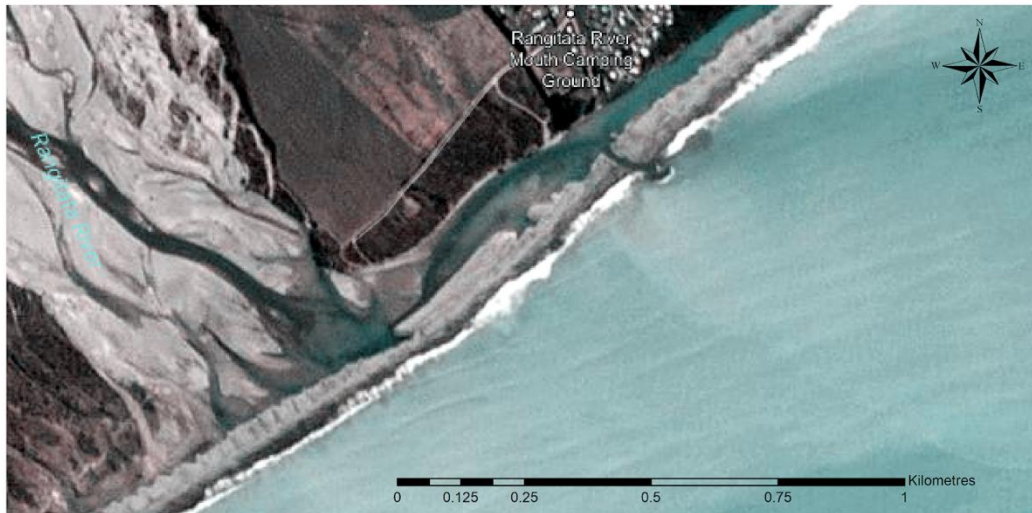


Figure 24. Image demonstrating the river channel flowing further into the usual hāpua location. This may be a possible reason for the shape of the bank erosion seen south-west of the Rangitata Huts. Image sourced from Planet Labs.

6.4.2 Erosion south of the river mouth

RCN1548, south of the river mouth, has been eroding since 1989 (Figures 6 and 7). This is due to sediment deposited at the coast and high-energy waves (Hart, Marsden, & Francis, 2008). The Rangitata River is considered a small river (Kirk, 1991). This means that the amount and type of sediment deposited at the coast is insufficient to maintain the coastline against the high-energy waves and longshore transport (Zenkovich, 1967). The Rangitata River typically deposits fine sediments that are transported by waves into the nearshore (Hart, Marsden, & Francis, 2008). The dominant northern longshore current (Apx. D3) also transport sediment away from RCN1548 which is contributing to the long-term erosional trend. Therefore, geomorphic variability in the RRME includes erosion south of the river mouth.

6.5 River Flow Influence

6.5.1 Flood Events

A barrier bar may experience significant morphological changes in response to high-energy flow events (Hart, 2009; Kirk, 1991; Masselink et al., 2014). It is common for barrier bars become truncated forming a wide outlet in a new position at RRME (Figure 15). A primary or secondary breach can be observed after high-flow conditions (Figures 15 and 16) (Apx. C)

which is similar to what Hart (2009) found at the Waitaki River mouth. The average river flow seen to breach the bar is $\sim 200 \text{ m}^3/\text{s}$ which is comparable to Todd (1991), however this is subject to other influences (Hart 2009). The primary driver of increased river flow rates is linked to increased precipitation (Li & McGregor, 2017) (Apx. F).

Low magnitude floods referred to as ‘freshes’ by Todd (1998) are less than $200 \text{ m}^3/\text{s}$. Freshes are generally not strong enough to cause a primary breach of the barrier bar. A secondary breach during a fresh is commonly seen at the northeastern end of the RRME. These events are most hazardous to the Rangitata Hut residents as the water backs up within the hāpua and causes increased flooding adjacent to the settlement.

A trend discovered following high flow events is the generation of a convex shape of the barrier bars (Figure 16). In the discussed flood examples, the seaward movement of the barrier bars surrounding the outlet was caused by deposition of sediment along the bars (Jowett, Richardson, & Bonnett, 2005).

6.5.2 Low flow events

Low flows at river mouths can cause closure of the river outlet, (Kain, 2009) and separate the hāpua from the river channel. However, barrier bar closure events are not common at the RRME and if they do occur, they are short-lived, lasting from hours (Measures et al. 2020) to days (Todd, 1998). It was difficult to identify full barrier bar mouth closures in the imagery from 2016-2020, however, a closure may still have occurred. Todd (1998) found that three short duration outlet closure events at the RRME occurred in June and July 1984, with a residual flow of around $10\text{-}30 \text{ m}^3/\text{s}$. The Rangitata River has had a low flow range of around $32\text{-}52 \text{ m}^3/\text{s}$ over the last 41-years, suggesting it has not reached the threshold for outlet closure. Other factors that influence outlet closure tend to be a combination of southerly waves, low flow in winter (Apx. E4), and large offsets of the river channel to the outlet (Todd, 1998). There were also many occurrences of the hāpua closing off from the main river channel, which tended to occur between $40\text{-}70 \text{ m}^3/\text{s}$. The impacts of river flow are essential when creating a baseline study of the RRME because they have such a range of different effects.

6.7 Outlet migration

The prevalence of southerly waves in the Canterbury Bight generates movement of sediment along the shoreline in a northward direction (Kirk 1991; Leckie, 1994;). This can influence the river outlet position (Todd, 1998). An outlet migration of 800m over four months was identified in imagery (Figure 18). Comparisons with wave data highlighted that the dominant wave direction during this time was from the south. The beach excursion and sediment volume plots (Figures 6 and 12) further cement the interpretation that the northern longshore current is the driving influence of the northern outlet migration (Paterson et al., 2001). Outlet migration was also observed by Hart (2009) and linked this to “periods of wave dominance” (Pg. 1358) or during periods of low flows and low energy waves.

7. Limitations

The river flow and wave data provided some limitations for this research. The data source locations are inadequate for identifying conditions at the RRME. Thus, flow and wave conditions at the hāpua will differ from their source. Furthermore, there were gaps in these datasets. There were also issues when it came to synthesising results due to each data set being recorded over irregular periods. The beach profiles were measured annually but at during different months. Between 1998 and 2006 there were no available aerial images, making trend identification difficult. During digitisation it was difficult to determine tide stage, exact flow, and differences between wet sand or shallow water due to georeferencing issues and poor resolution.

8. Conclusion

The RRME is dynamic and dominated by a hāpua. Fluvial and marine processes are the main drivers of geomorphic variability. This research project created a baseline study of the RRME. Similar studies have not been completed for some time and changes to the environment are inevitable. Data used for this analysis was aerial imagery, beach profiles, wave data, and river flow data. Key elements of geomorphic variability found through this study is a northward migration of the outlet channel, breaching of the barrier bar during flood events, erosion to the south of the river mouth, and accretion in the north. These trends can now be incorporated in an understanding of the normal variation seen at the RRME.

9. Further research

Conducting a baseline study for the RRME has created a reference point to guide future research. Focusing on controls outside of this research scope such as tides, tectonic uplift, and erosion rates may add value to future studies of the RRME. Further monitoring of climate change aspects may lead to changes in research methods and approaches. Finally, consistent and reliable image sources showing variations could be advantageous for continued research.

10. Acknowledgements

We would like to acknowledge our supervisor, Seb Pitman for his help and guidance throughout this research. We would also like to recognise our community partner, Justin Cope for bringing forth this research and for his advice and input throughout. Lastly, we would like to acknowledge Bruce Gabites for the data he supplied.

11. Appendices

Appendix A

Mixed-sand and Gravel (MSG) Beaches

The Rangitata Hāpua is located along a MSG beach. Storms are key drivers of morphological change on MSG beaches (Losada et al., 2016). Losada et al. (2016) found that during a storm, a concave beach face developed and the berm, which is in the foreshore during low energy conditions, was eroded. Overall, it is suggested that the profile of the barrier changes with respect to a balance between marine and fluvial processes (Hart, 2009; Kirk & Lauder, 2000; Measures et al., 2020; Single, 2011).

Appendix B

Beach profile analysis

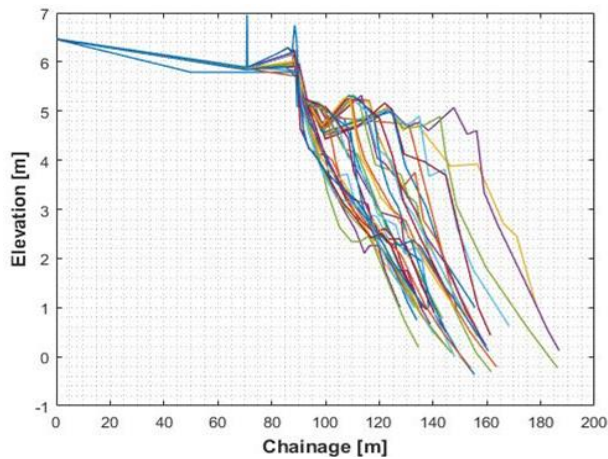


Figure B1. Beach envelope for RCN1548 for 1981 to 2019, which shows the minimum and maximum extent of the beach face. This envelope demonstrates that this site has experienced no change in profile shape over the years on record. Data

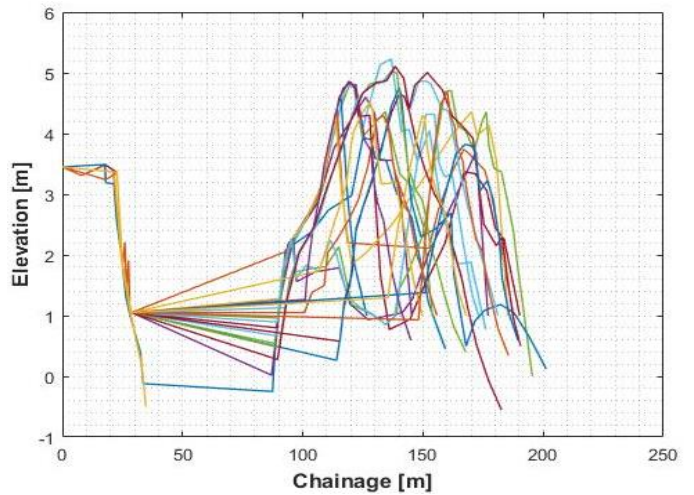


Figure B2. Beach envelope for RCN1782 1993-2019.

One main channel, which is the hāpua, can be identified between approximately 30m and 110m.

Data sourced from ECan.

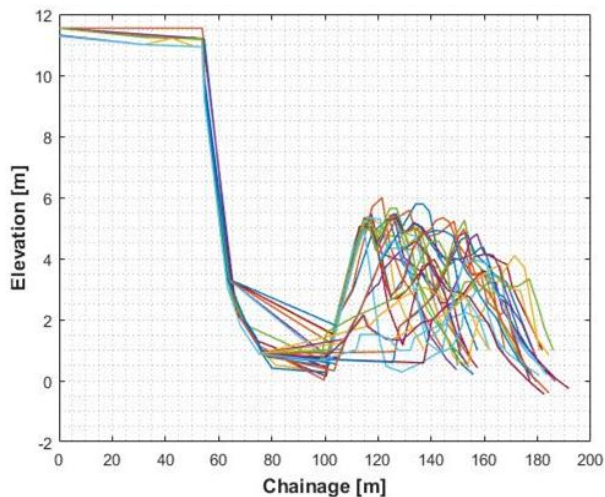


Figure B3. Beach envelope for RCN1830 1986-2019. One main channel, which is the hāpua, can be clearly identified. Data sourced from ECan.

Appendix C

Summary of Observed Features Before, During and After Two Flood Events

The below tables are observations made of the two flood events discussed in this report. Other floods were analysed but these were the chosen representative examples. Data sourced from ECan and Planet Labs.

Table C1. Table showing observations and measurements of the Dec 2019 flood sequence of a maximum flow of 2248m³/s. The largest observed changes from this flood was the convex shape the barrier bars formed as they moved seaward during this event. There was significant erosion noted SW of the northern huts.

Date of analysed image	River flow (average for the day in m ³ /s)	Hāpua closed or open?	Channel location (north, central or south)	Channel width	Bar width at beach profile RCN1782
BEFORE: 24 th November	71	Closed	Central	2 openings both 80m each	50m
DURING: 9 th December	720	Open	Central	440m	50m
AFTER: 23 rd December	91	Closed	Central	70m	50m

Table C2. Table showing observations and measurements of the November 2018 flood sequence of a maximum flow of 1847m³/s. The largest observed changes from this flood the barrier bar breaching directly downstream of main river flood and therefore moved outlet channel to a central position. Similar to the Dec. 2019 flood, the barrier bars moved seaward after the flood.

Date of analysed image	River flow (average for the day in m ³ /s)	Hāpua closed or open?	Channel location (north, central or south)	Channel width	Bar width at beach profile RCN1782	Volume of barrier bar(s) at RCN1782
BEFORE 1 st Nov	74	Open	North (far north)	20m	25m	No profiles completed in 2018
DURING 6 th Nov	112 (max flow on the 9 th at 1847)	Open	Central and north	60m north 340m Central	40m	15 March 2017 153.81
AFTER 9 th Nov	1421	Mostly closed	Central	50m	30m	11 April 2019 145.57

Appendix D

Analysis of wave data

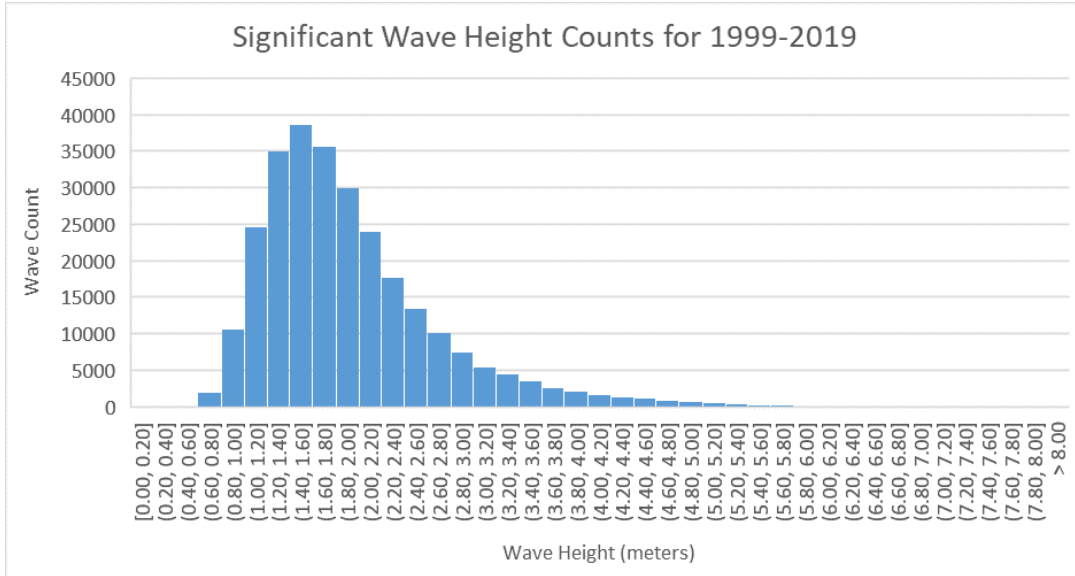


Figure D1. Histogram showing significant wave height counts recorded for 1999-2019. The most common waves (20,000 or more) consisted of heights ranging from 1 metre to 2.2 metres.

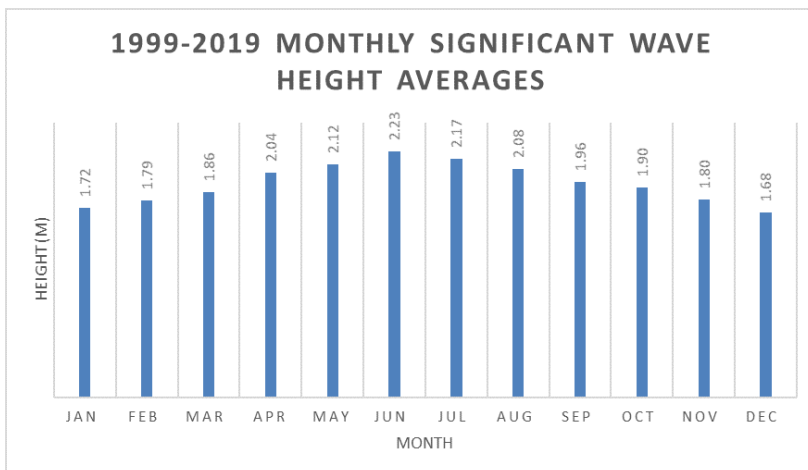


Figure D2. Bar chart showing the monthly significant wave height averages from 1999-2019. June and July feature the highest monthly averages of 2.23 and 2.17 respectively.

Table D3. Table showing wave direction and significant wave height annual averages for 1999-2019. The average wave direction is from the south-west and this aligns with the work of Pickrill & Mitchell (1978) who found that the east coast of the South Island of New Zealand is battered by mostly southerly swells, although the mixed wave climate also brings some northerly and easterly waves shoreward.

Year	Direction averages (Degrees)	Significant wave height averages
1999	147.20	1.78
2000	150.47	2.20
2001	150.59	1.90
2002	156.11	2.42
2003	149.28	2.15
2004	149.31	2.09
2005	139.70	1.91
2006	149.92	1.96
2007	151.71	1.92
2008	139.63	2.05
2009	143.82	2.10
2010	142.82	1.98
2011	144.86	2.13
2012	143.68	1.95
2013	139.19	1.88
2014	145.01	2.04
2015	152.35	2.12
2016	147.32	1.83
2017	143.40	1.91
2018	140.23	1.94
2019	146.54	1.94
Average	146.34	2.01

Appendix E

Analysis of river flow

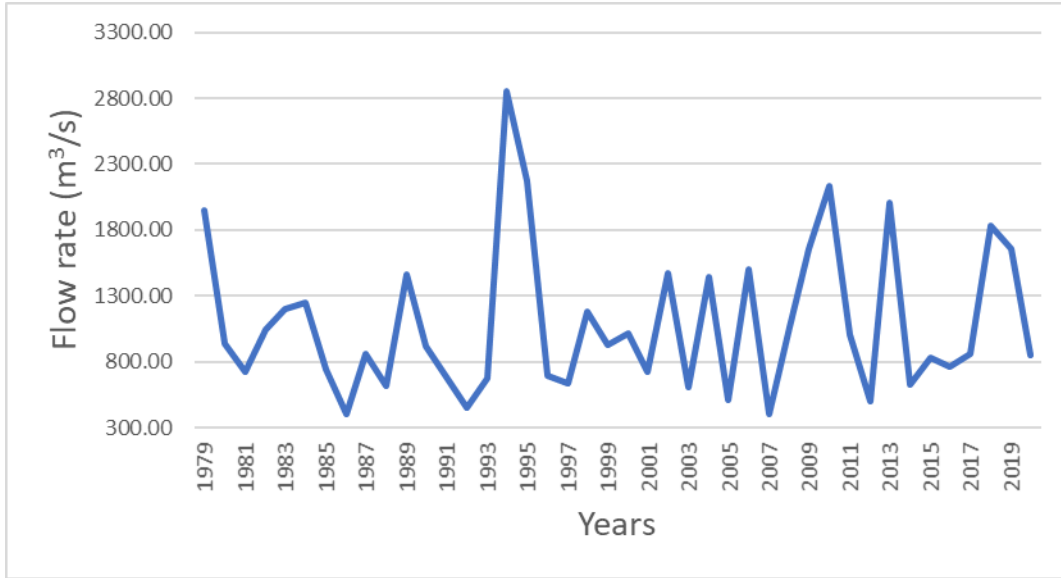


Figure E1. Graph showing annual high river flow averaged over the three largest events per year from 1979-2019. It shows a peak in high flow during 1994-1995. Data sourced from ECan.

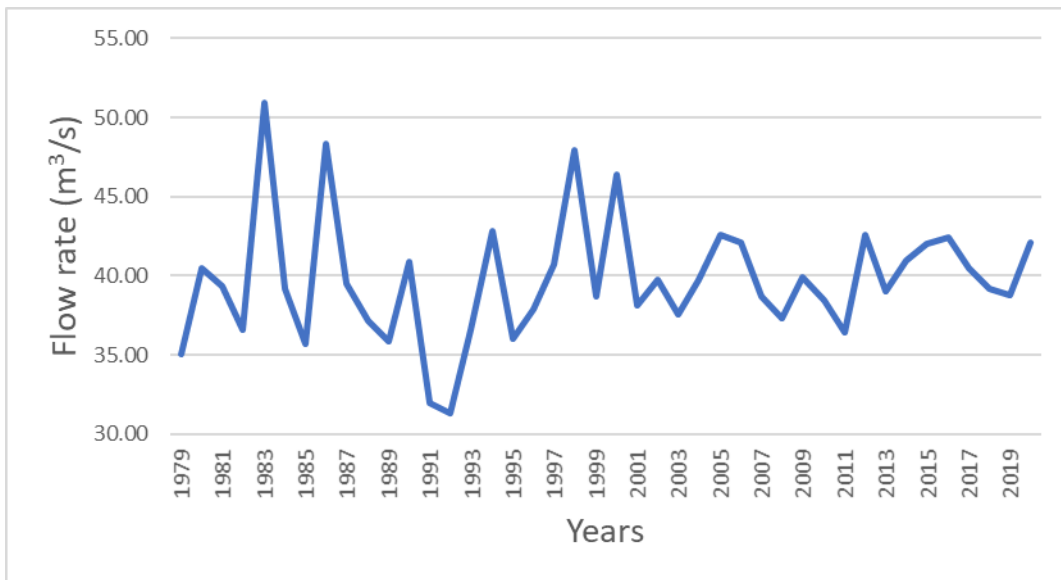


Figure E2. Graph showing annual low river flow averaged over the three smallest events for each year. It shows fluctuations in flow rate between 32 and 52 m³/s over the 41-year period. The lowest flow occurred from 1991-1992. Data source is ECan.

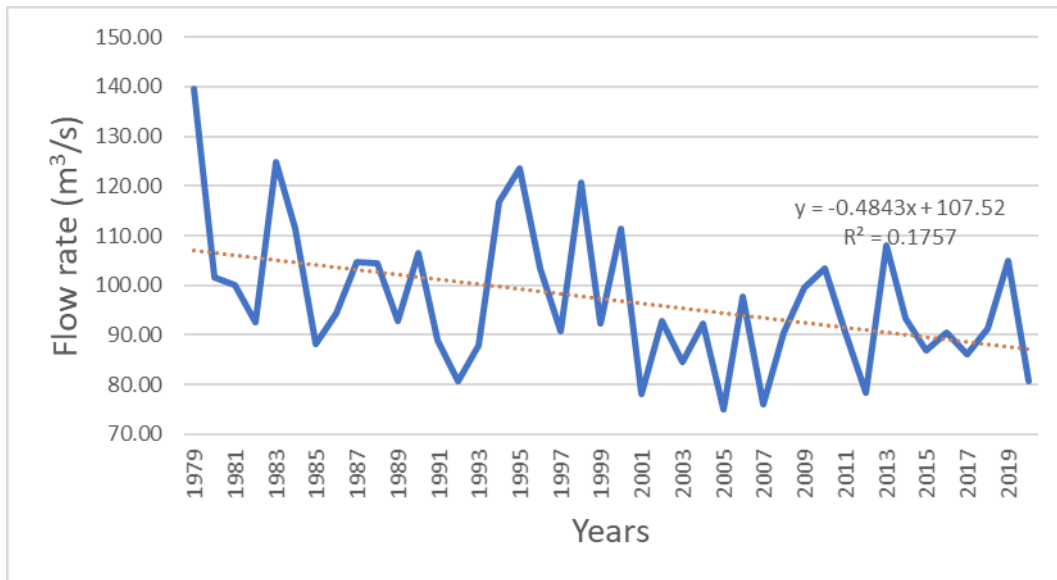


Figure E3. Graph showing annual average river flow. Fluctuates between 75-140 m³/s with an overall decrease in flow rate since 1979. Data source is ECan.

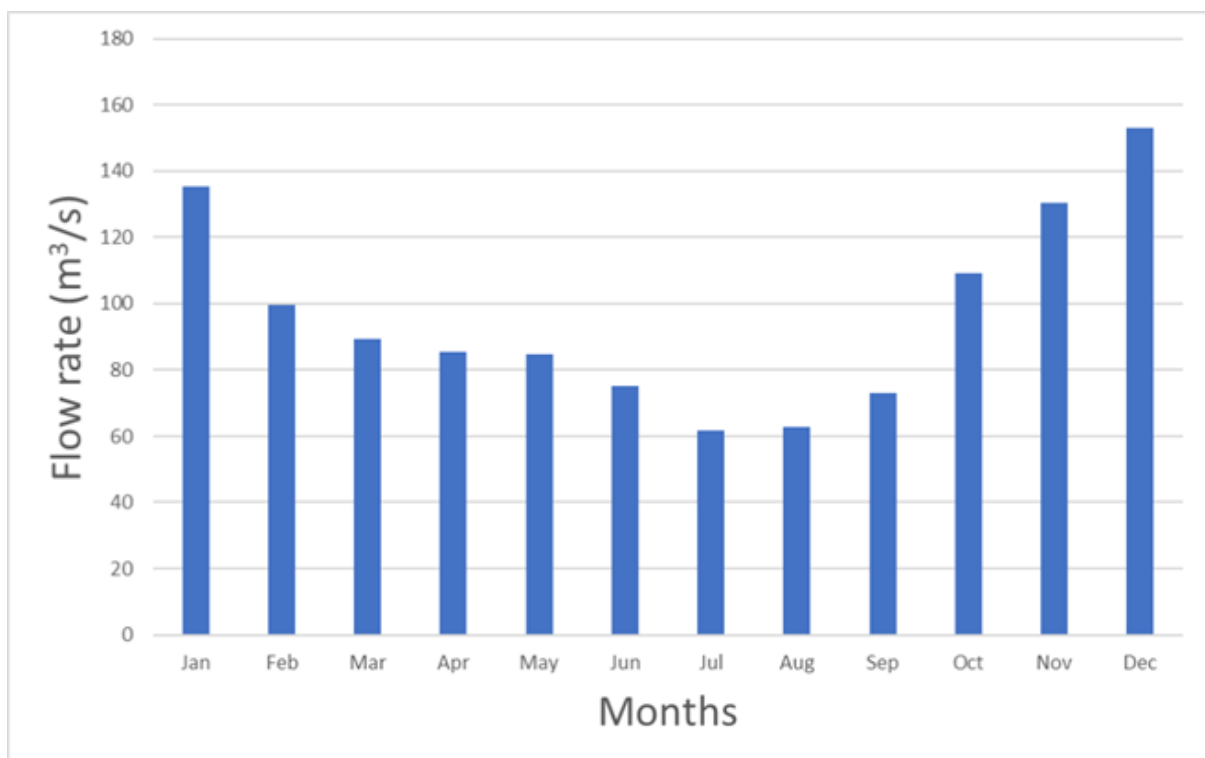


Figure E4. Graph showing average monthly river flow. The months of higher river flow are October through to February whereas July represents the month of lowest average flow. Data source is ECan.

Table E5. Table showing the mean flow, mean minimum flow and mean max flow for each year from 1979 to 2020. All measurement is in cubic meters per second. Data sourced from ECan.

Year	Mean flow	Mean min flow (Over 3 lowest events)	Mean max flow (Over 3 largest events)
1979	139	35	1949
1980	101	40	940
1981	100	39	725
1982	93	37	1044
1983	125	51	1205
1984	111	39	1251
1985	88	36	741
1986	94	48	403
1987	105	39	862
1988	104	37	613
1989	93	36	1465
1990	106	41	914
1991	89	32	684
1992	81	31	452
1993	88	37	679
1994	117	43	2854
1995	124	36	2174
1996	103	38	698
1997	91	41	639
1998	121	48	1179
1999	92	39	930
2000	111	46	1010
2001	78	38	721
2002	93	40	1472
2003	85	38	607
2004	92	40	1442
2005	75	43	506
2006	98	42	1499
2007	76	39	399
2008	91	37	1061
2009	100	40	1653
2010	103	38	2129
2011	91	36	1010
2012	78	43	500
2013	108	39	2006
2014	93	41	629
2015	87	42	827
2016	91	42	761
2017	86	40	862
2018	91	39	1831
2019	105	39	1657
2020	81	42	853
Average of years	97	40	1091

Appendix F

Rain and river flow for two flood events

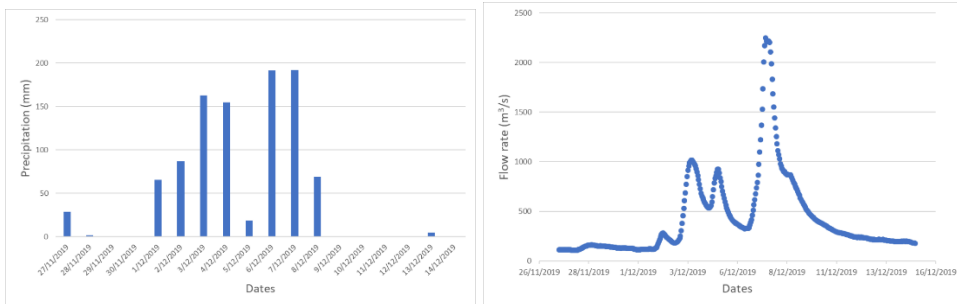


Figure F1. Rainfall at Mistake Flats Rain Gauge (December 2019) and Rangitata River flow at Klondyke for the associated period. Data source is ECan.

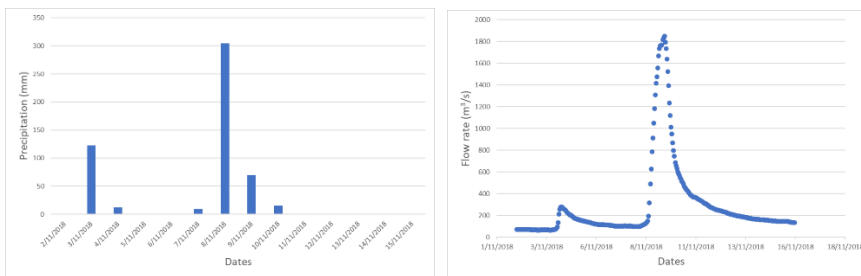


Figure F2. Graphs showing rainfall at Mistake Flats Rain Gauge (November 2018) and Rangitata River flow for the corresponding week. Data source is ECan.

Appendix G

Qualitative and quantitative analysis of imagery

Visual observations and measurements were used to compile Table F1 while further interesting observations are noted in Figure F2.

Table G1. Table showing observations made for the available images between 1937 and 2020 excluding images from Planet Labs. Data sourced from ECan, Planet Labs, Retro Lens and Google Earth pro.

Date	Source of image	River flow in m ³ /s	Barrier bar(s) closed or open to ocean?	Hāpua closed or open to river flow?	Channel location (north, central or south of main river flow)	Outlet channel width	Bar width at beach profile RCN1782 location
6th Oct 1937	Retro Lens	No data	Open at north end	Open	North	20m	45m
9th Sept 1954	Retro Lens	No data	Slightly open at mid-hāpua length	Open. Located in the south	North	20m	35m
31st Oct 1965	Retro Lens	No data	Open at mid-length hāpua	Open Located in the south	North	40m	20m, then bar cut by channel (20m wide), then 20.5m on the other side
19th Aug 1967	Retro Lens	No data	Open at central	Closed Small southern hāpua	Central	135m	30m
19th Feb 1977	Retro Lens	No data	Slightly open at north	Open	North	50m	25m
22nd Feb 1987	Retro Lens	68	Open central	Closed In far north east	Central	35m	35m
11th Nov 1998	Retro Lens	96	Open at 2 places	Open	Central (two outlet channels)	170m & 100m	40m, small inlet between 2 bars, then 30m
8th July 2009	Google Earth Pro	40	Mostly closed	Open	Central angle-parallel to coast	45m	30m

10th Aug 2020	Planet Labs	No data	Barely open	open	Central but slightly north	Unmeasurable as so small <8m.	45m
1st Dec 2011	Google Earth Pro	105	Open at north end	Open	North	30m	40
26th Feb 2012	Google Earth Pro	90	Open at north end	Open	North	25m	50m
17th Feb 2013	Google Earth Pro	60	Open	Mostly closed	South	20m	45m
26th Aug 2013	Google Earth Pro	45	Open	Open	Central	25m	65m
19th Oct 2015	Google Earth Pro	140	Open at North end	Open	North	35m	25m (Split bar)
29th Aug 2016	Google Earth Pro	45	Mostly closed	Open	South	5m	25m (Spilt bar)
4th Nov 2018	Google Earth Pro	210	Open at North end	Open	North	50m	40m
20th May 2019	Google Earth Pro	70	Mostly closed	Mostly closed	Central	10m	70m
6th June 2019	Google Earth Pro	85	Open	Mostly closed	Central	65m	25m

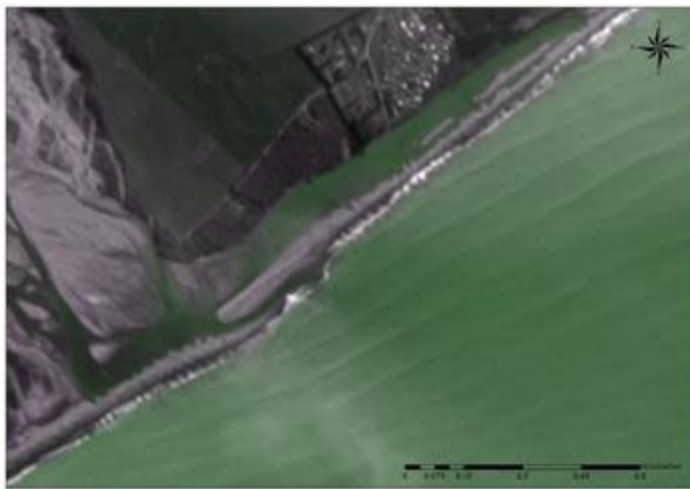


Figure G2. Map in false colour showing scalloped foreshore and lobed backshore with large south-easterly waves. Image sourced from Planet Labs.

Appendix H

Bank erosion

Table H1. This table represents the measured amount of erosion between the available images from 2009 to 2019. There are significant errors with these measurements due to the accuracy of the measuring tool, low resolution images combined with human error. There is a 5m plus or minus range associated with each measurement. Images sourced from Google Earth

Date	Erosion distance between this year and the following in metres at the greatest point (m)
2009 July	10
2011 November	10
2013 August	10
2015 October	2
2017 October	10
2019 June	-
2009-2019	35m at greatest point. Note: No erosion directly in front of huts